IAEA Neutronics Benchmark for EBR-II SHRT-45R

B. Vezzoni[1], W.F.G. van Rooijen[2], T. Fei[3], Y. Zhang[4,•], M. Marchetti[1], P.Balestra[5], C. Parisi[5]

[1]Karlsruhe Institute of Technology, Eggenstein - Leopoldshafen, Germany
[2]Research Institute of Nuclear Engineering (RINE), University of Fukui, Tsuruga, Japan
[3]Argonne National Laboratory, Argonne, Illinois, USA
[4]Paul Scherrer Institute, Villigen PSI, Switzerland
[5]Italian National Agency for new technologies, energy and sustainable economic development, ENEA, Casaccia research Center, Italy

E-mail contact of main author: barbara.vezzoni@kit.edu , rooijen@u-fukui.ac.jp

Abstract. Within the Coordinated Research Project (CRP) initiated by the International Atomic Energy Agency (IAEA) for investigating Shutdown Heat Removal Tests (SHRT) at Experimental Breeder Reactor II (EBR-II), an optional neutronics benchmark has been defined for providing reactivity feedback coefficients for the thermal hydraulic analysis of SHRT-45R. Several institutes participated in this benchmark, including: Karlsruhe Institute of Technology (KIT), University of Fukui, Paul Scherrer Institute (PSI), Argonne National Laboratory (ANL) and the Italian National Agency ENEA. Several stochastic and deterministic codes were used for this purpose. The results obtained in general were in good agreement. Remained discrepancies have been underlined and discussed in the present paper.

Key Words: Neutronics benchmark, EBR-II, Reactivity Feedback Coefficients.

1. Introduction

A Coordinated Research Project (CRP) initiated by the International Atomic Energy Agency (IAEA) aimed to benchmark Shutdown Heat Removal Tests (SHRT) conducted at Experimental Breeder Reactor II (EBR-II) [1,2]. Two SHRT tests (SHRT-17 and SHRT-45R) representative, respectively of Protected Loss of Flow (PLOF) and Unprotected Loss of Flow (ULOF) transients were considered. The SHRT-45R benchmark included both safety analyses and an optional neutronics benchmark for SHRT-45R. Only the activities carried out for the neutronics benchmark are described in this paper.

The objective of the neutronics benchmark was to provide reactivity feedback coefficients for the thermal hydraulic analysis of SHRT-45R. Several institutes participated in this benchmark, including: Karlsruhe Institute of Technology (KIT), University of Fukui, Paul Scherrer Institute (PSI), and Argonne National Laboratory. Later on, the Italian National Agency for new technologies, energy and sustainable economic development (ENEA) joined the study.

Several parameters were compared: keff, βeff, reactivity feedback coefficients (axial, radial and control rod expansion, sodium density, and Doppler) and the power distribution in each subassembly, including fission and gamma heat. The fission and decay heat power for 15 minutes after a postulated scram at the beginning of SHRT-45R were also calculated.

In the study, stochastic and deterministic codes were used: MC2-3/TWODANT, DIF3D, VARI3D, and PERSENT by Argonne, Serpent by PSI, and the ECCO/ERANOS codes by the University of Fukui and by KIT. KIT also used the PARTISN code and ENEA adopted MCNP6 and PHISICS codes.

In general, the results obtained by the participants are in quite good agreement. Results obtained for keff and βeff show a maximum difference of 1.2%. The reactivity feedback coefficients initially showed a large spread that was reduced by establishing consistency

• Note: Dr. Y. Zhang is actually working at KTH Royal Institute of Technology (Sweden)

among the definitions used by the participants. However, some spread remains, partially due to the different linear thermal expansion coefficients used in converting the change in reactivity (pcm) to change in reactivity per change in temperature (pcm/K), as discussed later. Differences due to core modelling options (detailed fuel pin modelling vs. homogenized subassembly modelling) and neutron cross-section preparation were also analysed.

Concerning the power distributions large discrepancies (up to 80%) were observed in the non-fuelled subassemblies, where photon heating dominates, while differences were less than 5% in the fuelled subassemblies. No recorded data are available for the detailed power distribution.

2. NEUTRONICS BENCHMARK DESCRIPTION

SHRT-45R is one of the tests conducted at the EBR-II plant to demonstrate the passive safety of a sodium fast reactor (SFR). This unprotected loss-of-flow (ULOF) test was conducted at the end of EBR-II Run 138B, during which EBR-II had been operated at 18 MW for 4.0 days and 60 MW (almost full power) for 1.6 days. The operating and design data for EBR-II Run 138B used for the benchmark exercise are shown in Table I.

The fuel form used for Run 138B was a metallic uranium-fissium alloy with ~67% U235 enrichment. The detailed fuel composition at the beginning of Run 138B was extracted from the Physics Analysis DataBase (PADB) [4] for each driver and blanket fuel assemblies divided into three axial burnable regions. Then a depletion calculation was performed by REBUS-3 [5] to calculate the fuel composition for every burnable region at the start of the test, i.e. at the end of Run 138B.

TABLE I: Design and operating data for EBR-II Run 138B [1-3]

Parameter	Value
Power (MW)	18 MW for 4 days and 60 MW for 1.6 days
Inlet temperature (K)	616
Outlet temperature (K)	716
Subassembly data at 20ºC (driver/blanket)	
Subassembly pitch (cm)	5.89
Na gap thickness (mm)	0.38
Duct wall thickness (mm)	1.02
Structural material	SS316/SS304
Lower shield height (cm)	55.32/3.46
Fuel height (cm)	34.29/139.70
Gas plenum height (cm)	24.90/11.348
Upper shield height (cm)	38.69/0.0
Pin data at 20ºC (driver/blanket)	
# pins	91/19
Fuel slug diameter (cm)	0.34/1.11
Cladding inner diameter (cm)	0.38/1.16
Cladding outer diameter (cm)	0.44/1.25

Several subassembly types were loaded in core for Run 138B of EBR-II as indicated in *FIG. 1*. The inner core zone (inner 7 rows of the core) was loaded by driver fuel subassemblies and it was surrounded by about 3 – 4 rows of steel radial reflectors. Several rows of blanket fuel subassemblies were located outside the radial reflectors. The driver fuel subassemblies (*FIG. 2*) were composed by regular drivers (subassembly contained 91 fuel pins, *FIG. 2-a*) and half-

worth driver (HW driver SA containing 46 fuel pins and 45 steel pins, *FIG. 2-b*). There were two types of control/safety subassemblies: a) regular control subassembly similar a regular driver subassembly but contained only 61 fuel pins located inside an inner duct (*FIG. 2-c*), b) a high-worth control subassembly that in addition contains a poison region consisted of 7 B_4C pins above the fuel zone. The control and safety subassembly insertion was measured to be 21.06 and 15.97 cm, respectively.

The parameters considered in the benchmark study are reported in Table II together with the description of the assumed calculation procedure following ANL recommendations. The adoption of common calculation procedure led to a reduction of discrepancies among participants that were observed during the first "blind" calculation phase [3].

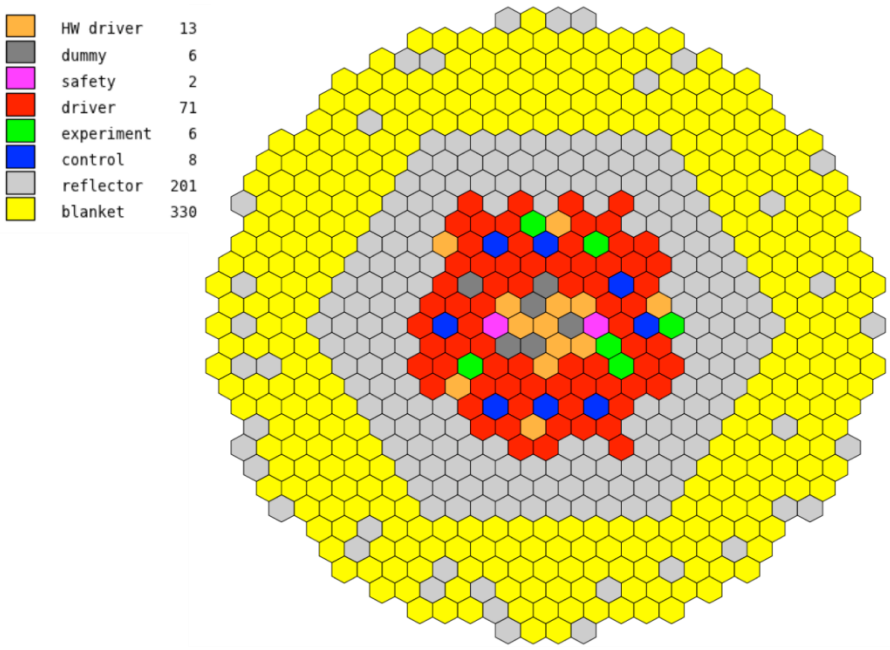

FIG. 1. EBR-II Core Loading Pattern for Run 138B [3].

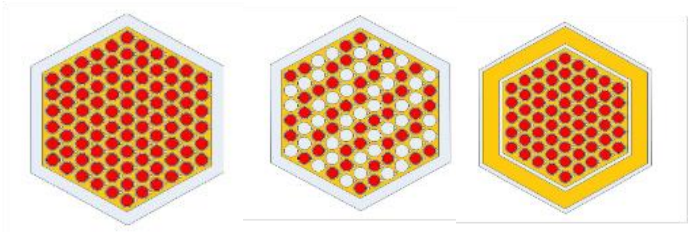

(a) (b) (c)

FIG. 2. EBR-II drivers: a) regular driver, b) half-worth driver, c) regular control subassembly.

3. METHODOLOGY

Different stochastic and deterministic neutronics tools and methodologies were employed by the benchmark participants. A summary of the reactor analysis codes and of the cross-section (XS) library used by each participant is shown in Table III. In the following, a short description of the codes and methods used by each participant is reported.

3.1 Karlsruhe Institut of technology (KIT)

The reference option considered at KIT is the ECCO/ERANOSv2.2 codes with 3D HEX-Z model and transport calculations run using the variational nodal method (VARIANT).

Different options included an equivalent XYZ model (e.g. suitable for calculations with the PARTISN code) have been considered.

TABLE II: EBR-II SHRT-45R: parameters considered according to benchmark specifications

Benchmark results	**Definitions**
Core multiplication factor	-
Effective delayed neutron fraction	-
Axial expansion reactivity feedback coefficient	Calculated assuming that the active fuel height increases by 10% in the driver SAs, XX09, HW-CR, and SR, while the fuel and structural material number densities are reduced by 10% in the active fuel region of these SAs.
Radial expansion reactivity feedback coefficient	Calculated assuming that the SA pitch is increased by 1%, while the number densities of all isotopes excluding sodium in all regions are divided by 1.01^2.
Sodium density reactivity feedback coefficient	Calculated assuming that sodium density decreases by 10% in all the regions of all SAs.
Doppler reactivity feedback coefficient	Calculated assuming that fuel temperatures in the driver SAs, XX09, HW-CR, and SR are doubled. It has been calculated as $K_D/\Delta T$.
Control rod expansion reactivity feedback coefficient	Calculated as k_{eff} vs. control/safety rod insertion.
Power distribution for each SA	-

TABLE III: List of XS library and codes used by each participant.

Participant	**XS Library**	**Code**
KIT (Germany)	JEFF-3.1	ERANOS2.2 [6], PARTISN[7]
University of Fukui (Japan)	JENDL-4.0u, JEFF-3.1.2, ENDF/B-VII.1	ERANOS2.0
PSI (Switzerland)	JEFF-3.1.1	Serpent [8]
ANL (U.S.A.)	ENDF/B-VII.0	MC^2-3/TWODANT[9], DIF3D[10], PERSENT[11], MCNP6[12]
ENEA (Italy)	ENDF/B-VII	MCNP6[12], SCALE 6.1.2 release [13], PHISICS, version under development (alpha testing) [14]

It has been decided to limit the numbers of different burnable zones in the model for further comparison with the SIMMER code. Therefore, six average compositions representative of six burnable zones have been determined by axial (subassemblies specific axial weighting factors obtained by normalizing the U235 lumped Fission Products) and radial (on power/subassemblies provided) averaging of the provided compositions. For those burnable zones, effective cross sections have been produced by means of the ECCO code (JEFF3.1 nuclear data library) assuming subassemblies heterogeneous description and 1968 energy groups before collapsing to 33 energy groups effective neutron-cross sections for transport analysis. For the non-burnable zones (reflectors, dummy, etc.), cross sections have been processed in the same way but considering subassemblies homogeneous description.

Feedback coefficients have been evaluated by direct calculations. A parametric study on the sodium density reactivity coefficient has been performed [15]. The effective delayed neutron fraction has been evaluated with an extended version of the ERANOS code for 3D HEX-Z geometry.

3.2 University of Fukui

The ERANOS v2.0 analysis software was used in combination with three cross section libraries based on modern sets of evaluated nuclear data: JENDL-4.0, JEFF-3.1.2 and ENDF/B-VII.1. As specified by the benchmark, effective cross sections were generated for fission products as well as the "fissium" part of the fuel. Since the EBR core contains several types of fuel assemblies, cell calculations were performed for each SA type with the ECCO module (1968 / 33 energy groups, 2D heterogeneous geometry). Non-fuel mixtures were treated as infinite homogeneous mixtures in 33 energy groups. Equivalent cross sections for the control rods were prepared with the reactivity equivalence method. The microscopic cross sections from the cell calculations were combined with the isotopic densities from the benchmark to make macroscopic cross sections for the core calculations.

Core calculations were performed in Hex-Z geometry with the nodal PN-method (TGV-VARIANT module). For thermal expansion feedback, the core materials were grouped into solid and liquid materials. Radial and axial expansion is calculated assuming that all solid materials, including the metallic fuel, expand as cladding. Expansion of the coolant is independent. The reactivity effect of thermal expansion was calculated directly, i.e. with core calculations at the reference and at elevated temperature; no attempt was done to use perturbation theory. Delayed neutron data was taken from the JENDL-4.0 evaluated files and reformatted for use in ERANOS. The effective delayed neutron fraction was calculated with diffusion theory in Hex-Z geometry.

3.3 Paul Scherrer Institut (PSI)

Serpent is a continuous energy Monte Carlo code that was initially developed by the Technical Research Centre in Finland. As other Monte Carlo codes, the configuration of sub-assemblies or whole reactor core in Serpent can be described in two or three dimensions by using universe based geometrical models. Neutron transport is simulated with the Woodcock Delta-tracking method. The burnup calculation is done by solving the Bateman equation with the Transmutation Trajectory Method (TTA).

Regions in different types of assemblies loaded with fuel, absorber, steel or blanket pins were modeled heterogeneously by defining different lattices in the Serpent model, in order to achieve better calculation accuracy. Other regions, such as coolant inlet or outlet region, were simply modeled homogeneously. Another major simplification is that blanket assemblies in the Serpent model were loaded with the same fuel composition. Isotopic compositions of this blanket fuel were averaged by fuel composition in the assemblies located at the inner-most and outer-most rings.

The hexagonal 3D full-core Serpent calculations produced the effective multiplication factor (keff), the effective delayed neutron fraction (βeff), safety related reactivity coefficients, as well as the power distribution throughout the core.

3.4 Argonne National Laboratory (ANL)

MC2-3/TWODANT was employed to generate the multi-group neutron and photon cross section, the neutron and photon kerma factor, and the photon production matrix. A two-step calculation procedure was employed to generate the cross section. In the first step, fine-group (1041) neutron flux spectra in different core regions were obtained based on a simplified R-Z

model of the EBR-II core for Run 138B. Then in the second step, these region-wise flux spectra were used to condense the neutron cross section to 33 groups for each region.

Both diffusion nodal method and variational nodal method (VARIANT module of DIF3D) were employed to calculate the k-eff, the neutron and photon heating power distribution in the core. The photon heating power distribution was obtained in three steps. The first step solved the neutron flux distribution, which generated the photon source by multiplying the photon production matrix. The second step obtained the photon flux distribution by solving the fixed source problem. At last, the photon flux was multiplied by the kerma factor to give the photon heating power. The reactivity feedback coefficients were evaluated by the PERSENT codes.

3.5 Italian National Agency for new technologies, energy and sustainable economic development (ENEA)

The reference tool chosen to calculate the EBR-II cross sections by ENEA was SCALE6.1.2 [13]. The 238-group cross section library based on ENDF/B-VII was selected. The CENTRM module was used for the self-shielding calculations. CENTRM calculates problem-dependent, group-averaged cross sections, using as weight the flux calculated by solving the 1D Boltzmann transport equation with a continuous-energy cross section library. For the present work, a 33-energy group structure, used also by the ERANOS code, was used for the few-groups homogenization.

Since EBR-II has a heterogeneous core structure, many different 2D SCALE models were used to calculate the final cross section library. The "B1" critical spectrum search option was used after the transport calculations to generate the homogenized constants. The 97 core subassemblies were modelled using 75 collapsed compositions. Three layers were used for taking into account the axial burnup and temperature variations.

In addition to MCNP6 [12], the PHISICS code [14] based on variational nodal method, was used. Models with hot and cold dimensions and compositions were assessed.

4. RESULTS

4.1 keff and βeff

The eigenvalue of the core (keff) and the effective delayed neutron fraction (βeff) predicted by all participants are listed in Table IV. In general, the keff values range from 0.9849 to 0.9923, range of about 740 pcm, considering same conditions, i.e. transport approximation and expanded dimensions and compositions. The ENEA PHYSICS, the PSI Serpent and KIT PARTISN model evaluated keff to be about 1000 pcm than other results, and this was mainly caused by the difference in the core modelling (dimension and fuel composition at 20°C). Larger values are achieved by ENEA MCNP6 and PHYSICS (hot dimensions). The diffusion solver of DIF3D employed by ANL also significantly underestimated the keff by ~2000 pcm when comparing to other transport solvers. The same effect has been found by KIT as indicated in [15]. Other differences may come from the heterogeneous/homogeneous treatment of XS, by the solver, by the way adopted for modelling the core (HEX-Z vs. XYZ); all points analysed during the study. The results on βeff are in very good agreement as indicate din Table IV.

4.2 Reactivity feedbacks

A summary of the reactivity feedbacks is shown in Table V. The values obtained by the participants adopting the definitions in Table II are in good agreement. Some variations remain. The methods employed and the thermal expansion coefficients used to convert the change in reactivity (pcm) to change in reactivity per change in temperature (pcm/K) are the dominant effects of those variations.

Axial and radial reactivity feedback coefficients show standard deviation is ~20% and ~15% respectively, when excluding the results from ANL diffusion calculation. The variations in these two reactivity feedback coefficients were partially due to use of different thermal expansion coefficient to convert pcm to pcm/K. If using the same thermal expansion coefficient, the standard deviation is reduced to ~10% for both cases.

The sodium void reactivity feedback coefficients predicted in different cases agreed well with a standard deviation of ~13%. No specific definition (concerning the zones to be included in the simulation) has been provided initially in the benchmark for the sodium density reactivity feedback coefficient. A parametric study has been performed at KIT [15]. Depending on the option considered, the values obtained show a difference of almost 50%.

TABLE IV: Comparison of keff and βeff for EBR-II benchmark.

Participants	Cases	k_{eff}	β_{eff}
ANL	Diffusion	0.9670	7.05E-03
	VARIANT	0.9885	7.05E-03
	MCNP6	0.9904	-
University of Fukui	JENDL-4.0u	0.9923	6.91E-03
	JEFF-3.1.2	0.9850	7.02E-03
	ENDF/B-VII.1	0.9849	7.08E-03
KIT	ERANOS	0.9876	6.91E-03
	PARTISN (Sn=16)	1.0034	-
PSI	Serpent	1.0007±0.00008	6.94E-03±0.00012
ENEA	MCNP6	0.99667±0.00007	6.85E-03±0.00010
	PHISICS (Hot dimensions)	1.00004	6.94E-03
	PHISICS (Cold dimensions)	1.00612	6.92E-03

TABLE V: Comparison of reactivity feedback coefficients for EBR-II benchmark.

Participants	Cases	Reactivity feedback coefficient (pcm/K)			
		Axial Expansion	Radial Expansion	Sodium Void	Doppler
ANL	Diffusion	-0.36	-1.78	-1.70	-0.06
	VARIANT	-0.65	-1.67	-1.49	-0.05
University of Fukui	JENDL-4.0u	-0.84	-2.10	-1.90	-0.02
	JEFF-3.1.2	-0.85	-2.14	-2.02	-0.02
	ENDF/B-VII.1	-0.85	-2.15	-1.89	-0.02
KIT	ERANOS (VARIANT)	-0.68	-2.42	-2.15	-0.04
PSI	Serpent	–0.48±0.04	–1.72±0.03	–1.68±0.05	–0.05±0.005
ENEA	MCNP6	-0.514±0.003	-1.605±0.027	-1.813±0.041	-0.06±0.020
	PHISICS (Hot dimensions)	-0.44	-2.26	-2.36	-0.07
	PHISICS (Cold dimensions)	-0.58	-1.73	-1.61	-0.07

The fuel Doppler feedback coefficients have larger spread. This is mainly due to the different ways to calculate this coefficient used by the participants. However, the Doppler effect is two order of magnitude lower than the other reactivity effects (see Table V)..

The effect of CR expansion has been determined by calculating the keff as a function of control rod insertion. *FIG. 3* shows the keff as a function of control rod insertion after re-normalizing the keff for no control rod insertion. The general shape of the curves agrees well. When control subassembly is fully inserted, the VARIANT based calculation produced a larger keff than Serpent calculation. This is due to axial source convergence problem. The EBR-II control subassembly was loaded with fuel pins. When it was inserted, the active fuel region of the control subassembly would move out of the active core. Higher order axial source expansion is required to accurately predict the axial flux distribution in the control subassembly.

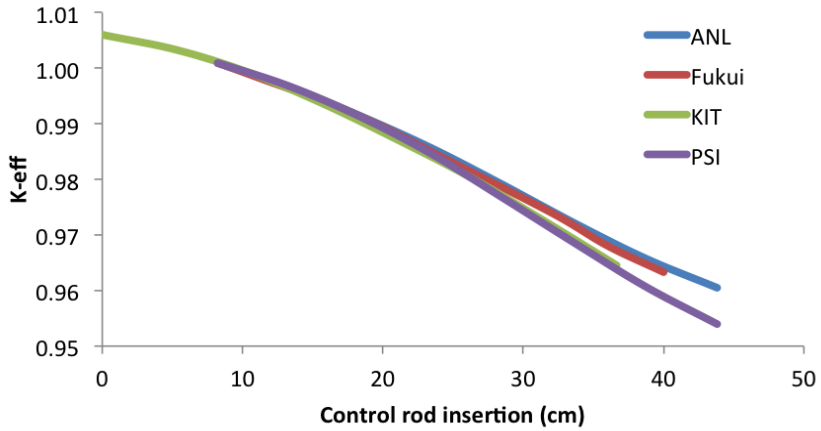

FIG. 3. Control rod driveline expansion reactivity feedback

4.3. Power Distribution

The total power (neutron + photon) per SA has also been analysed by the benchmark. *FIG. 4* shows the predicted values for the core zone (inner 7 rows). Good agreement was observed for the driver subassemblies (most <5%) among all participants. Larger differences were observed in the dummy (steel) subassemblies, reflectors and XX10 (experiment subassembly). In these subassemblies, more than 80% power was produced through photon heating. Simplified treatment of the photon flux has been considered at KIT by employing the ERANOS KERMA_CORRECTION module that allows reducing the initial discrepancies of 20%. Different results have been obtained by University of Fukui using the KERMA_CORRECTION module in ERANOS2.0 [16]. The calculation models adopted by PSI and ENEA did not include photon heating calculation, thus the power in the dummy, reflector, and XX10 subassemblies was not shown in *FIG. 4* for the PSI and ENEA results.

Other differences are due to difference in the EBR-II core model as in the case of dummy subassembly in which different mass of steel has been considered and for control and safety subassemblies in which the difference is related to the subassembly axial position. However, due to the lake of knowledge about the way in which the power distribution provided in the benchmark was calculated, it is not possible to draw clear conclusions on the comparison.

5. CONCLUSIONS

The CRP on EBR-II SHRT-17 and SHRT-45R initiated by IAEA aimed to validate state-of-the-art SFR safety and neutronics analysis codes and to train the next generation of SFR analysts and designers. For the SHRT-45R test benchmark two parts was considered safety transient analysis and neutronics benchmark. The optional neutronics benchmark focused on the evaluation of the reactivity feedback coefficients useful for the safety analyses.

The results obtained for keff and βeff predictions were in good agreement while the reactivity feedback coefficients predicted by all participants showed some spread. The differences come mainly by the different linear thermal expansion coefficients used in converting the change in reactivity (pcm) to change in reactivity per change in temperature (pcm/K) and to the core modelling options adopted (detailed fuel pin modelling vs. homogenized subassembly modelling). The SA-wise power distribution was also compared. Large differences of power were observed in the structural subassemblies (dummy, reflector, XX10, etc.) where photon heating power is dominant.

The overall study has allowed further validating via a code-to-code comparison the tools and methods adopted by the different participants. The parametric studies carried out by the participants have provided further inside on understanding the discrepancies obtained.

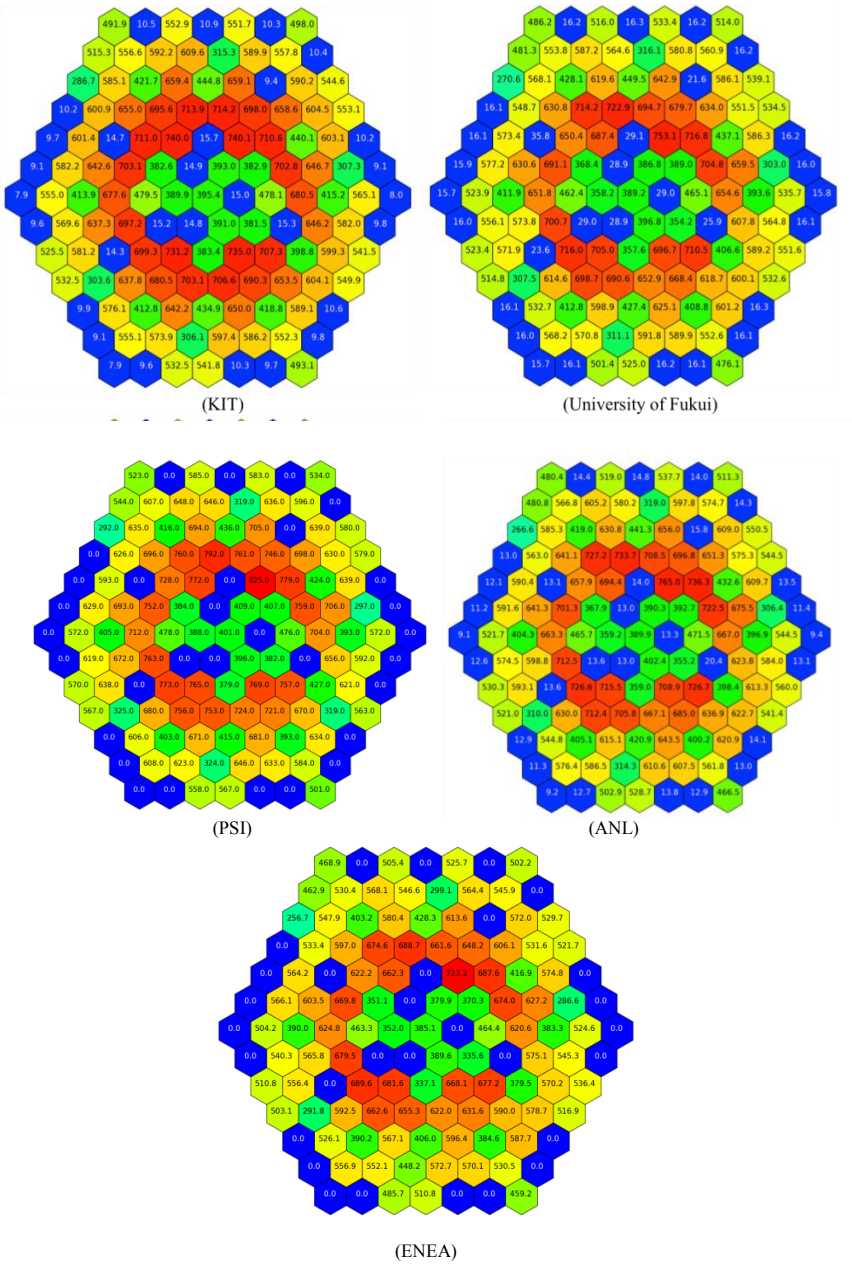

FIG. 4. Power map in the inner 7 rings of EBR-II core in Run 138B (power in each subassembly is in unit of kW).

Acknowledgments

The authors would like to thank IAEA for sponsoring the activity and for the support provided.

References

[1] BRIGGS, L., et al, "Benchmark Analyses of the Shutdown Heat Removal Tests Performed in the EBR-II Reactor," *Proc. FR-13*, Paris, France, March 4–7, International Atomic Energy Agency, (2013).

[2] BRIGGS, L., et al, "EBR-II Passive Safety Demonstration Test Benchmark Analyses – Phase 2," NURETH-16, Chicago, IL, August 30 – September 4, (2015).

[3] FEI, T. et al., "Neutronics Benchmark for EBR-II Shutdown Heat Removal Test SHRT-45R", Proc. Int. Conf. PHYSOR 2016, Sun Valley, Idaho, USA, May 1 – 5, (2016).

[4] FEI, T. et al., "Review of the IFR Physics Analysis Database," 2014 ANS annual meeting, Reno, U.S.A., June 15-19, (2014).

[5] TOPPEL, B. J., "A User's Guide to the REBUS-3 Fuel Cycle Analysis Capability," ANL-83-2, Argonne National Laboratory (1983).

[6] RIMPAULT, G., et al., "The ERANOS Code and Data System for Fast Reactor Neutronic Analysis," Proc. Int. Conf. PHYSOR 2002, Seoul, Korea, October 7-10, (2002).

[7] ALCOUFFE, R. E. et al., "PARTISN: A Time-Dependent, Parallel Neutral Particle Transport Code System," LA-UR-08-07258 (2008).

[8] LEPPÄNEN, J., "Serpent - a Continuous-energy Monte Carlo, Reactor Physics Burnup Calculation Code", Technical Research Centre of Finland, (2015).

[9] LEE, C. H. and YANG, W. S. "MC^2-3: Multigroup Cross Section Generation Code for Fast Reactor Analysis," ANL/NE-11-41 Rev. 1, Argonne National Laboratory (2011).

[10] DERSTINE, K. L., "DIF3D: A Code to solve One-, Two- and Three-Dimensional Finite-Difference Diffusion Theory Problems," ANL-82-64, Argonne National Laboratory, April (1984).

[11] Smith, M. A., et al., "VARI3D & PERSENT: Perturbation and Sensitivity Analysis," Argonne National Laboratory, ANL/NE-13/8, June 15, (2013).

[12] PELOWITZ, D.B. "MCNP6™ User's Manual," LA-CP-11-01708, Los Alamos National Laboratory, (2011).

[13] BOWMAN, S. M., "SCALE 6: comprehensive nuclear safety analysis code system", Nuclear Technology, Special Issue on the SCALE Nuclear Analysis Code System/Reactor Safety 174 dx.doi.org/10.13182/NT10-163 (2011).

[14] RABITI, C., et. al., "New Simulation Schemes and Capabilities for the PHISCS/RELAP5-3D Coupled Suite", Nuclear Science and Engineering, Vol. 182, pp. 104-118 (2016), dx.doi.org/10.13182/NSE14-143.

[15] VEZZONI, B., et al., "IAEA EBR-II Neutronics Benchmark: Impact of Modeling Options on KIT Results", Proc. Int. Conf. PHYSOR 2016, Sun Valley, Idaho, USA, May 1 – 5, (2016).

[16] VAN ROOIJEN, W.F.G., "Analysis of the EBR-II SHRT-45R neutronics benchmark with ERANOS-2.0", Proc. Int. Conf. FR17, Yekaterinburg, Russian Federation, 26 – 29 June 2017.